New Phytologist

Research

# Stand density and local climate drive allocation of GPP to aboveground woody biomass

**Steven A. Kannenberg[1], Flurin Babst[2,3], Mallory L. Barnes[4], Antoine Cabon[5], Matthew P. Dannenberg[6], Miriam R. Johnston[6] and William R. L. Anderegg[7,8]**

[1]Department of Biology, West Virginia University, Morgantown, WV 26506, USA; [2]School of Natural Resources and the Environment, University of Arizona, Tucson, AZ 85721, USA; [3]Laboratory of Tree-Ring Research, University of Arizona, Tucson, AZ 85721, USA; [4]O'Neill School of Public and Environmental Affairs, Indiana University, Bloomington, IN 47405, USA; [5]Swiss Federal Institute for Forest, Snow and Landscape Research WSL, Birmensdorf, Switzerland; [6]Department of Geographical and Sustainability Sciences, University of Iowa, Iowa City, IA 52242, USA; [7]School of Biological Sciences, University of Utah, Salt Lake City, UT 84112, USA; [8]Wilkes Center for Climate Science and Policy, University of Utah, Salt Lake City, UT 84112, USA

Author for correspondence:
*Steven A. Kannenberg*
*Email: steven.kannenberg@mail.wvu.edu*

Received: *3 October 2024*
Accepted: *8 January 2025*

*New Phytologist* (2025)
**doi**: 10.1111/nph.20414

**Key words:** allocation, carbon storage, dendrochronology, eddy covariance, forest, gross primary productivity, tree growth.

## Summary

- The partitioning of photosynthate among various forest carbon pools is a key process regulating long-term carbon sequestration, with allocation to aboveground woody biomass carbon (AGBC) in particular playing an outsized role in the global carbon cycle due to its slow residence time. However, directly estimating the fraction of gross primary productivity (GPP) that goes to AGBC has historically been difficult and time-consuming, leaving us with persistent uncertainties.
- We used an extensive dataset of tree-ring chronologies co-located at flux towers to assess the coupling between AGBC and GPP, calculate the fraction of fixed carbon that is allocated to AGBC, and understand the drivers of variability in this fraction.
- We found that annual AGBC and GPP were rarely correlated, and that annual AGBC represented only a small fraction (*c*. 9%) of fixed carbon. This fraction varied considerably across sites and was driven by differences in stand density and site climate. Annual AGBC was suppressed by *c*. 30% during drought and remained below average for years afterward.
- These results imply that assumptions of relatively stationary allocation of GPP to woody biomass and other plant tissues could lead to systematic biases in modeled carbon accumulation in different plant pools and thus in carbon residence time.

## Introduction

Forests play a crucial role in the cycling and sequestration of carbon and serve as a sink for up to a quarter of anthropogenic carbon dioxide emissions annually (Bonan, 2008; Pan *et al.*, 2011). However, understanding the future evolution of the land carbon sink, including the allocation within different pools and their residence times (Friend *et al.*, 2014; Pugh *et al.*, 2020), remains among the largest uncertainties in future carbon cycle projections (O'Sullivan *et al.*, 2022). As such, there has been a tremendous amount of research quantifying the fluxes and pools of forest carbon using a variety of methods, each with their respective strengths and weaknesses. Eddy covariance, for instance, provides high-frequency measurements of the net land-atmosphere carbon exchange but at a relatively small (and geographically biased) number of sites and with no direct ability to estimate within-stand allocation of that carbon. By contrast, forest inventories provide on-the-ground measurements of stand structure and tree size, but are generally conducted infrequently. Tree rings provide annually resolved measurements of stem radial growth over decades to centuries but often contain within- and among-site sample biases that preclude direct estimation of woody net primary production (Nehrbass-Ahles *et al.*, 2014). Given the complementary strengths and weaknesses of these approaches, the integration of tree biometric measurements, dendrochronology, and eddy covariance has emerged as a particularly promising way to quantify forest carbon cycling. Collectively, these approaches include well-established methodologies, multi-decadal scopes, and openly available datasets across hundreds of sites globally.

Critically, woody tree growth and forest carbon uptake are fundamentally different processes, and carbon dynamics inferred based on the measurement of one may not be consistent with dynamics inferred from the measurement of the other. These differences could arise due to a few nonexclusive mechanisms. First, growth and photosynthesis are sensitive to different environmental drivers. Depending on a wide array of factors, wood formation can sometimes be more limited by turgor pressure, and thus water availability, or by cold temperatures than by carbon availability from photosynthesis, which tends to be more sensitive to

fluctuations in light, temperature, leaf area, and the various drivers of stomatal conductance (Hsiao, 1973; Muller *et al.*, 2011; Peters *et al.*, 2021). Second, the different measurement methods of dendrochronology and eddy covariance may preclude direct comparison of growth and photosynthetic processes. Specifically, (1) ecosystem fluxes measured by eddy covariance include abiotic fluxes and a sometimes sizeable contribution of understory vegetation (Misson *et al.*, 2007), (2) tree selection and dendrochronological sampling are often biased toward serving the needs of individual studies (Nehrbass-Ahles *et al.*, 2014; Dye *et al.*, 2016; Babst *et al.*, 2018), and (3) uncertainty due to the complex post-processing of eddy covariance data (Loescher *et al.*, 2006). Finally, autotrophically fixed carbon is dynamically allocated to multiple sinks (e.g. coarse and fine roots, stems, leaves, sugars and starches, defense compounds, and exudates), and the nature of this allocation is highly variable at short timescales (Brüggemann *et al.*, 2011; Campioli *et al.*, 2011; Hartmann *et al.*, 2020). The drivers of these allocation processes are difficult to disentangle (Pugh *et al.*, 2020) and could introduce temporal lags that further mask potential links between tree growth and forest photosynthesis (Teets *et al.*, 2018b). Given these mechanisms, we should perhaps expect tree photosynthesis and growth to poorly covary at annual or sub-annual time scales, unless they are strongly co-limited by the same drivers in restrictive (e.g. cold and/or dry) environments.

There is indeed an emerging view that forest carbon uptake (gross primary productivity (GPP)) and tree growth are often decoupled (Körner, 2015; Cabon *et al.*, 2022). Moreover, various global change drivers, such as springtime warming (Keenan *et al.*, 2014; Dow *et al.*, 2022), elevated $CO_2$ (Walker *et al.*, 2020), and drought (Kannenberg *et al.*, 2019a,b, 2022), can further decouple temporal variability in stem growth from carbon uptake, likely due to the changes they cause in carbon allocation. Importantly, the degree to which growth and GPP are coupled may differ across space and time (Cabon *et al.*, 2024), necessitating a mechanistic understanding of when, where, and why these processes are linked. Extensive curated datasets of tree growth (e.g. the International Tree Ring Data Bank) and carbon flux observations (e.g. AmeriFlux, FLUXNET, and ICOS) do exist, but these measurements are infrequently co-located, precluding a comprehensive understanding of the linkages between these two processes.

Recent evidence of systematic growth–GPP decoupling has prompted a reexamination of the view that tree growth is commonly 'source-limited'. This perspective states that plant growth is not commonly limited by the availability of sugars or nonstructural carbohydrates, and is instead more limited by other environmental factors, such as temperature and water availability (Körner, 2015). The implications of this perspective for above- and belowground tree physiology are large (Prescott *et al.*, 2020), but the ramifications for the broader carbon cycle depend on the magnitude of GPP that is allocated to tree growth, since woody biomass is the longest-lived vegetative carbon pool in forests. Recent efforts have sought to estimate this fraction using tree rings (Babst *et al.*, 2014b; Pappas *et al.*, 2020; Teets *et al.*, 2022; Wei *et al.*, 2024), but these studies have had narrow geographic scope (less than five sites). Other studies, particularly the meta-analysis of Litton *et al.* (2007), have used direct measurements of the fraction of carbon uptake contained in aboveground growth across numerous sites, but such survey-based efforts are limited across longer time scales. Improving the spatial and temporal insights into allocation of GPP to woody biomass is necessary to gauge the confidence warranted in generalized C budgets for forests. These questions have wide-ranging implications for the forest carbon cycle given the long residence time of woody biomass, and thus its role in mediating the future evolution of the global carbon cycle (Carvalhais *et al.*, 2014; Pugh *et al.*, 2020). For example, many ecosystem models simulate allocation to tree growth using simplistic coefficients (Fatichi *et al.*, 2019) that are either static or change at a coarse timescale (Merganičová *et al.*, 2019), which tends to bias modeled estimates of forest carbon storage toward being more constant through time, despite the fact that allocation can be highly variable (Litton *et al.*, 2007). If the processes driving wood growth differ from those driving photosynthesis, assumptions of stationary carbon allocation based on source availability will lead to increasing biases in carbon residence time as hydroclimatic change potentially induces allocation away from aboveground woody biomass growth and toward other sinks, such as roots, defense, or respiration.

Here, we used an extensive dataset of 73 tree-ring chronologies collected within the footprint of 32 flux tower sites and comprising a total of 348 site-years of overlapping ring width and flux tower data. We developed a novel method to scale measurements of tree radial growth to species- and stand-weighted estimates of annual aboveground woody carbon increment (AWCI) that are comparable in space and time to GPP derived from eddy covariance. This method only requires estimates of species composition and stand basal area and can thus be easily applied at any other flux tower site where tree-ring chronologies have been collected. We ask three primary questions:

(**1**) To what degree are annual AWCI and GPP correlated?
(**2**) What fraction of GPP is allocated to tree-ring-derived AWCI (AWCI : GPP), and how does this vary across space and time?
(**3**) What are the primary drivers of interannual variability in AWCI : GPP, and how well can we predict AWCI : GPP?

## Materials and Methods

### Tree-ring and eddy covariance data

We used tree-ring and eddy covariance data from Cabon *et al.* (2022), which represents the most comprehensive dataset to date of tree-ring chronologies collected within the footprint of flux towers. This dataset comprises 32 flux tower sites and spans 73 chronologies across North America and Europe (Supporting Information Fig. S1; Table S1). These include annual measurements of ring width and monthly GPP, aggregated to current year, previous year, and water year (i.e. previous October to the current September) sums. The mean overlap period between tree-ring chronologies and GPP at these sites was 14 yr, with only four sites having an overlap period of < 10 yr. Many of

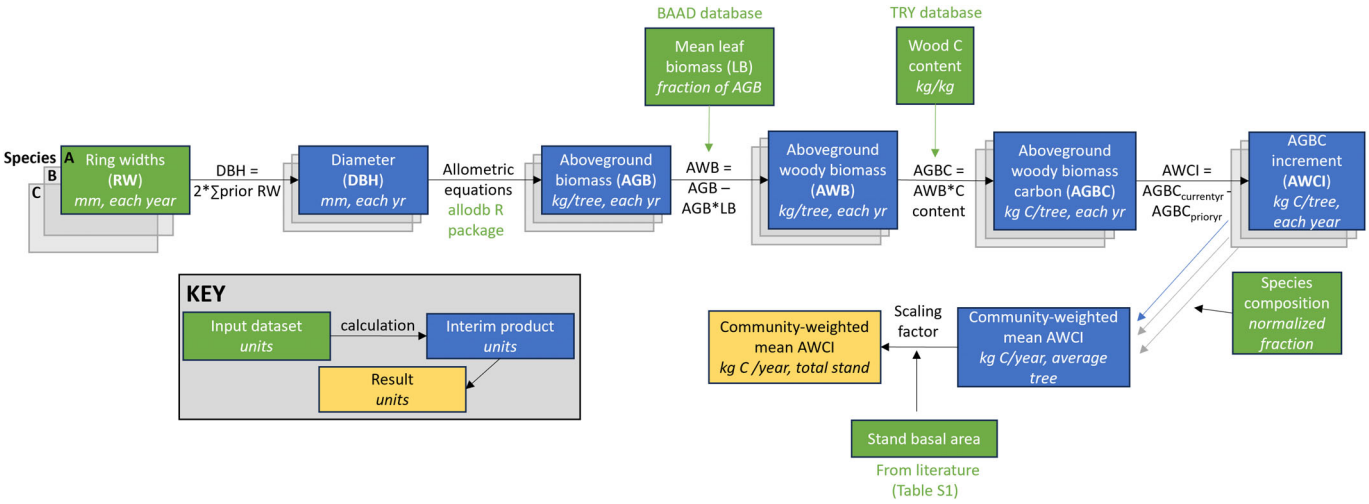


**Fig. 1** Schematic detailing the method for scaling measurements of tree-ring width to chronologies of aboveground woody carbon increment (AWCI).

these sites were sampled for tree cores in a systematic way to represent stand species and size distributions, while others targeted trees representative of those in the canopy. More details on data acquisition can be found in Cabon *et al.* (2022). In addition to the site metadata present in Cabon *et al.* (2022), available here in Table S1, we obtained MODIS-derived leaf area index (LAI, the 500 m resolution MCD15A2H product) for the grid cells containing each site using the R package MODISTOOLS (Tuck *et al.*, 2014) and aggregated it into annual growing season (May through September) means.

## Scaling from tree rings to aboveground woody biomass carbon

To directly compare the magnitude of absolute tree-ring widths (a unit of annual radial growth) with annual GPP (a flux of carbon on a per area basis), we generated time series of aboveground woody biomass carbon (AGBC) for each tree-ring chronology, weighted by species composition, and applied a scalar based on aboveground carbon density data at each site (Fig. 1). First, absolute ring widths were converted to diameter at breast height (DBH) by summing ring widths in all years before the target year and multiplying by 2. Because increment cores exclude outer bark and only occasionally extend to the pith, these 'inside-out' DBH estimates will frequently be biased low (Dannenberg *et al.*, 2020; Lockwood *et al.*, 2021), but our stand-level scaling procedure (Fig. 1) accounts for this bias as described below. This method also assumes that trees grow symmetrically (a common assumption in dendrochronology). Our cores were sampled to minimize asymmetry (e.g. by coring on perpendicular sides of the tree and avoiding growth irregularities), but this potential source of error is worth highlighting. Next, annual diameter reconstructions were converted into aboveground dry biomass using the R package ALLODB (Gonzalez-Akre *et al.*, 2022). *Allodb* relies on a large dataset of allometric equations for 701 tree species to derive aboveground biomass, while also weighting equation parameters for sample size and climatic/taxonomic similarity. Out of the 43 species in our dataset, species-level allometric equations were available for 34 species, and genus-level allometries were available for the remainder. Next, aboveground woody biomass was estimated by subtracting out leaf biomass, calculated using the mean percent leaf biomass attained from the BAAD database for each of our species (Falster *et al.*, 2015). Only field-derived allometries done on mature trees were considered for this analysis. When species-level values were not available, genus-level or family-level averages were used. Foliar allocation has been found to be fairly static across sites and years (Litton *et al.*, 2007), and furthermore significant relationships between tree DBH and foliar allocation were rare in our dataset (< 10% of sites). Thus, we believe using species means to be a reasonable assumption. Finally, aboveground woody biomass was converted to AGBC using mean species-specific wood carbon content values from the TRY database (Kattge *et al.*, 2020). When species-level values were not available, genus-level or family-level averages were used. AGBC was then converted into yearly increments (AWCI) by subtracting the previous year AGBC from the current year AGBC.

In total, this method calculated the mass of aboveground woody carbon that is contained in each chronology from raw measurements of ring width. However, multiple species are present at most flux tower sites and do not occur in equal abundance. In order to account for the presence of multiple species, we used species fractional abundance (percent of total stand basal area attributed to each species) estimates available at each site (Cabon *et al.*, 2022) to create community-weighted AWCI values for each site-year, and removed any site-years where not all species chronologies were present. These community-weighted AWCI values were still not appropriate to compare directly with GPP, though, since they are indicative only of the carbon contained in the cored trees. Therefore, AWCI chronologies needed to be converted to stand-level values. To do so, we searched the literature for estimates of stand basal area for each site (Table S1) and compared these values to estimates of community-weighted basal area contained in our chronologies to develop a scaling

factor that converts AWCI from the cored trees to a stand- and community-weighted estimate of AWCI. This stand scaling factor should also implicitly correct for any low-bias in ring-width-based DBH and AWCI. We only amassed literature stand basal area measurements during years near when flux data and tree-ring chronologies overlapped, and the scaling factor was created using our reconstructed basal area measurements that occurred closest to the year when basal area was directly sampled. While uncertainties are inherent in the use of allometric equations and stand basal area values, we note that these uncertainties are likely to be larger across sites than across years within a given site.

The use of basal area estimates from the literature, along with diameter reconstructions and other uncertainties detailed here, may cause noise and/or biases in our results. Therefore, we compared our AWCI estimates to those from Teets *et al.* (2022), which is the most comprehensive dataset of AWCI at flux tower sites to date that uses on-site stand surveys (as opposed to our literature-based values). First, in order to make their estimates of woody biomass increment (above- and belowground, including foliage) comparable to our AWCI estimates (aboveground woody biomass only), we subtracted out the mean percentages of foliage and root biomass (obtained via our BAAD-derived dataset) from the Teets *et al.* (2022) woody biomass increment estimates. We then compared our AWCI estimates with theirs across the 6 sites and 76 site-years that were present in both datasets. The two AWCI estimates were significantly correlated (Fig. S2; $P < 0.001$) and well-linked ($R^2 = 0.51$). Importantly, our AWCI estimates are only 2% higher on average than the Teets *et al.* (2022) estimates. Therefore, while we believe that there is much value in uncovering the mechanisms by which AWCI estimates may differ across methods, our approach is valid for understanding AWCI dynamics across a broader range of sites than was previously possible.

### Random forest analysis

To better understand the environmental drivers of AWCI, GPP, and the AWCI : GPP ratio, we conducted a random forest analysis using the R package RANDOMFOREST (Liaw & Wiener, 2002). Most predictor variables were previously compiled for each flux site (Cabon *et al.*, 2022) except for stand basal area, which was compiled from the literature (see Table S1) and LAI (described above). For each of the response variables – AWCI, GPP, and AWCI : GPP – we developed two types of random forest models: one focusing on interannual variability in the response variables and another on mean annual site-level values. These two model types were chosen to distinguish whether the drivers of AWCI, GPP, and AWCI : GPP were primarily due to temporal variability in meteorological conditions, or due to broader site-specific differences (e.g. mean climate or vegetation type/density).

To quantify the drivers of interannual variability in our response variables, we used growing season (May–September) climate data as predictors: climatic water deficit, precipitation, vapor pressure deficit, Palmer Drought Severity Index (PDSI), air temperature, incoming shortwave radiation, and LAI. Due to its high collinearity with other variables, climatic water deficit was excluded from the final model. The remaining predictors, which demonstrated low collinearity (correlation coefficient < 0.7), were retained (Dormann *et al.*, 2013). We normalized all climate variables by *z*-scoring (except for PDSI, which is inherently scaled) to account for variability in climatic conditions across sites.

At the site level, our predictors were site-specific characteristics and annual climate variables: IGBP vegetation classification, mean annual LAI, climatic water deficit (potential evapotranspiration minus actual evapotranspiration), precipitation, incoming shortwave radiation, air temperature, and stand basal area. We confirmed that none of these predictors were highly collinear (correlation coefficient < 0.7), and thus, all variables were retained in the final model (Dormann *et al.*, 2013).

Each model consisted of 500 decision trees, with the number of predictors sampled at each random forest split determined through k-fold cross-validation (five predictors produced the lowest cross-fold validation error for all models). To evaluate model performance, we partitioned the data into training (80%) and testing (20%) subsets, randomly resampling this division 100 times. We evaluated the predictive accuracy by applying models trained on the training subset to the testing subset. Variable importance for all predictors was calculated using the 'importance' function in RANDOMFOREST (which quantifies variable importance via the decrease in Gini impurity when using a particular variable to split the data), and we explored the relationships between model predictors and response variables by creating smoothed partial dependence plots using the R package PDP (Greenwell, 2017).

### Effect of pluvials, droughts, and drought legacies

To quantify the impacts of water stress on AWCI : GPP, we identified severe drought (PDSI < −3) and extreme pluvial (PDSI > 3) years within our dataset. Any drought/pluvial years that were also followed by a consecutive drought/pluvial were removed before analysis. The AWCI : GPP ratio was then compared between climatically normal years, droughts, pluvials, and for the 5 yr following drought.

### Statistical tests

Ordinary least squares regression was used to assess the relationship between AWCI and GPP (after confirming that the assumptions of linear regression were met), and two-tailed *t*-tests were used to compare differences among groups. The AWCI : GPP ratio was multiplied by 100 so that the resulting units are percentages. All statistical analyses were conducted in R v.4.3.1 (R Core Team, 2023).

## Results and Discussion

### Weak coupling of AWCI and GPP

Across all site-years, AWCI was significantly correlated with current year GPP, previous year GPP, and previous October to

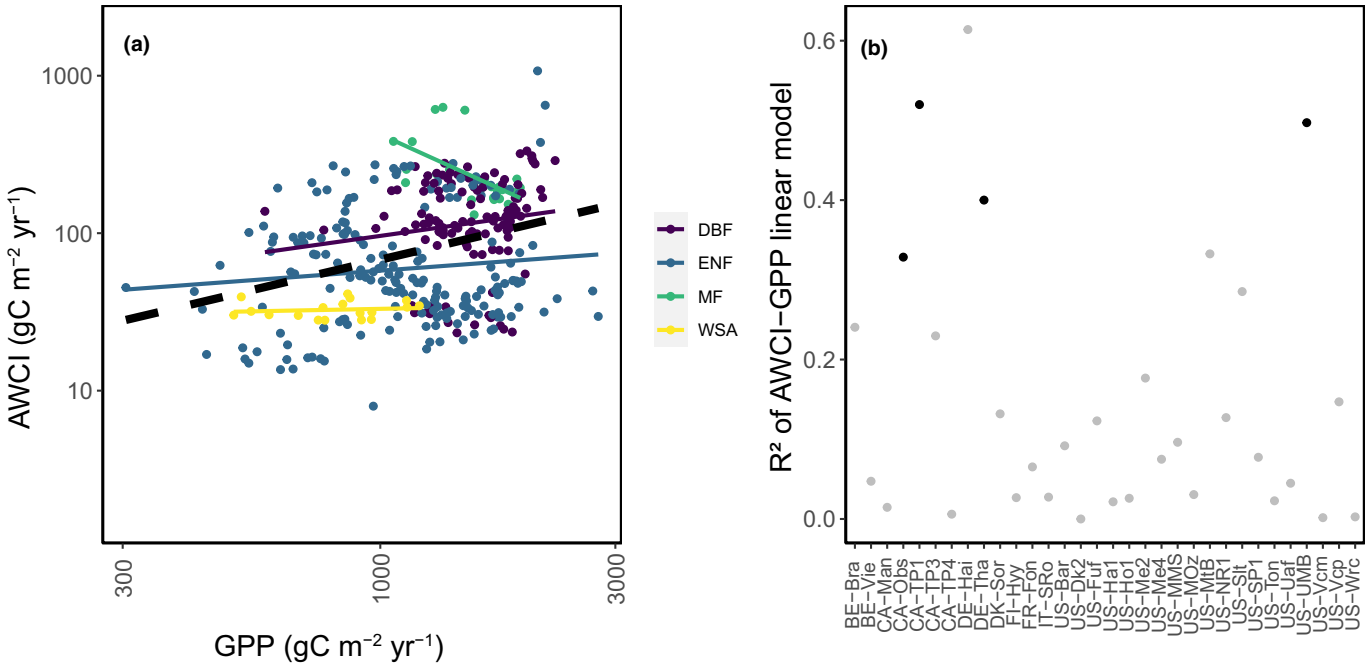


**Fig. 2** Relationships between aboveground woody carbon increment (AWCI) and gross primary productivity (GPP) (a), along with the coefficient of determination ($R^2$) of the linear relationship between AWCI and GPP at a given site (b). In (a), colored lines represent the linear model fit for all sites within a given IGBP classification, while the black dotted line represents the linear fit across all site-years. In (b), gray points represent nonsignificant relationships while black points represent significant relationships ($P < 0.05$). Both axes in (a) are plotted on a log scale for clarity, but see Supporting Information Fig. S9 for a nonlog transformed version.

current September GPP ($P < 0.001$), though the strength of these relationships was low ($R^2$ = 0.07, 0.08, and 0.07, respectively). The relationship remained weak when AWCI outliers (> 2 SD from the mean) were removed ($R^2$ = 0.06–0.08 for all GPP aggregations) and when only considering sites with at least 10 yr of overlap between chronologies and GPP ($R^2$ = 0.08–0.12). Therefore, for all subsequent analyses we only refer to current year GPP and include data across all sites. Within-site correlations between AWCI and GPP were also very low and largely nonsignificant (Fig. 2a,b), though there were certain sites where AWCI and GPP were moderately coupled. Within-site interannual variability in AWCI (mean coefficient of variation = 0.23) was comparable to that of GPP (mean coefficient of variation = 0.21); however, the coefficient of variation for mean AWCI across sites was 0.84 while it was only 0.32 for GPP. This indicates that AWCI and GPP are comparable in their temporal variability at a given site, but AWCI is substantially more variable across locations. This result expands upon previous research that tree-ring widths and GPP are quite decoupled by finding that GPP is also decoupled from AWCI, especially across sites.

Previous research has found contrasting evidence that tree growth and GPP can be linked at some sites (Teets *et al.*, 2018a, 2022; McKenzie *et al.*, 2021) and yet also can be decoupled at others (Rocha *et al.*, 2006; Delpierre *et al.*, 2016; Pappas *et al.*, 2020; Wei *et al.*, 2024). We found similar results across a much broader range of sites – the linkage between AWCI and GPP seemed to be poor generally, but can exist in some forests. It is worth noting that these processes have been found to be significantly correlated at some of the sites in our dataset (Teets *et al.*, 2022), though this study also found tree growth to be only loosely coupled to GPP across site-years. Moreover, other previous research has found a strong growth–GPP coupling at some of our Canadian plantation sites (McKenzie *et al.*, 2021), a result we also find here. This replication gives us confidence that our method of scaling ring width to AWCI results in robust estimates of whole-forest growth variability, especially in forests where species composition and allometry are well resolved.

## How much of GPP is allocated to AWCI?

Scaling tree-ring width chronologies to whole-stand woody biomass carbon allowed us to calculate the fraction of GPP that was allocated to AWCI on an annual scale. We found that this fraction was relatively small and highly variable across sites, with a mean value of 8.97% and a 5$^{th}$ to the 95$^{th}$ percentile range of 1.68–23.08% (Fig. 3). While this fraction varied interannually within a given site (mean coefficient of variation within a given site = 0.23), most of the variability in AWCI : GPP was cross-site (coefficient of variation across site means = 0.79). Higher cross- vs within-site variability in AWCI : GPP has been reported previously (Guillemot *et al.*, 2015; Rog *et al.*, 2024), and likely indicates that the drivers of AWCI : GPP are site-specific factors (e.g. fertility or age; DeLucia *et al.*, 2007; Vicca *et al.*, 2012) instead of interannual climate variability (to be described later for tests of this hypothesis). Given that many

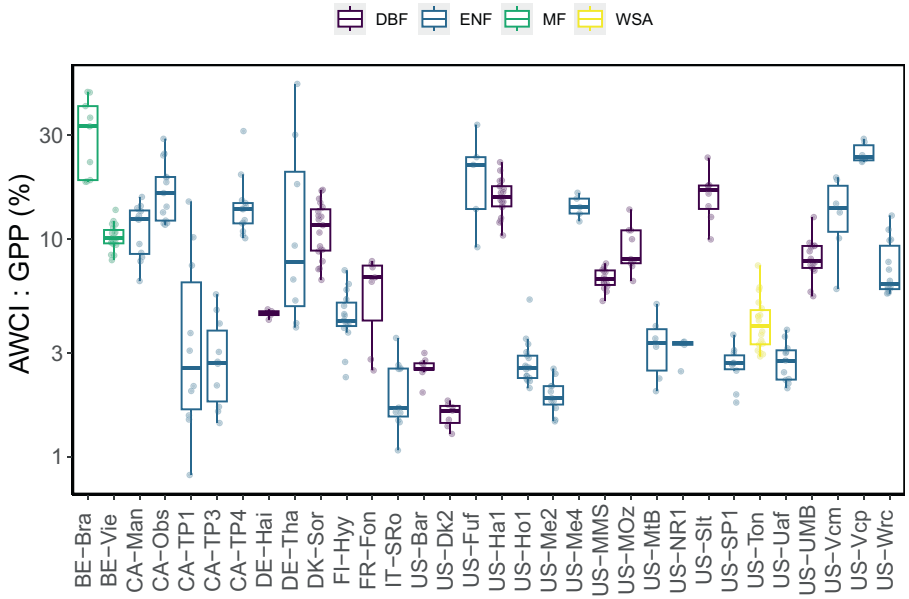


**Fig. 3** AWCI : GPP across sites. Each point represents a single site-year, color-coded by IGBP classification. Boxes represent the median ± the interquartile range, while the 'whiskers' indicate the maximum/minimum non-noutlier values. The *y*-axis is plotted on a log scale for clarity, but see Supporting Information Fig. S10 for a nonlog-transformed version. AWCI, aboveground woody carbon increment; GPP, gross primary productivity.

ecosystem models simulate wood allocation using simplistic coefficients that are derived from limited empirical data (Fatichi *et al.*, 2019), this result should prompt further investigation into the drivers of carbon allocation, as well as developing models of sink-driven processes (Cabon *et al.*, 2024).

The small magnitude of AWCI : GPP may be surprising, but it is within the range of previous estimates of forest carbon budgets. For example, a substantial fraction (*c.* 10–50%) of stand GPP may represent carbon fixed by understory species or small trees that are not represented in our dataset (Misson *et al.*, 2007; Ikawa *et al.*, 2015; Piponiot *et al.*, 2022). Of that remaining GPP, *c.* 50–60% is used for autotrophic respiration (Rog *et al.*, 2024), *c.* 10–20% is allocated to foliage (Falster *et al.*, 2015), and *c.* 25–50% is allocated to various belowground pools, such as root growth, mycorrhizas, and exudates (Litton *et al.*, 2007). Thus, while the fate of fixed carbon is highly variable across space and time, we contend that it is expected that AWCI represents only a small percentage of stand GPP.

However, some other studies have found higher AWCI : GPP percentages (*c.* 12–20%), especially when reconstructing AWCI using dendrometer and/or survey-based approaches (Litton *et al.*, 2007; Brzostek *et al.*, 2014; Babst *et al.*, 2014b; Finzi *et al.*, 2020; Teets *et al.*, 2022). As most of these other studies were able to directly quantify stand biomass with on-site measurements, we acknowledge that these discrepancies could have arisen due to uncertainty in our stand basal area estimates. However, we suggest that there is no reason to suspect that uncertainty in these data would produce a consistent underestimation of AWCI : GPP. There could also be biases associated with the lack of diameter measurements of the trees cored in our dataset (Lockwood *et al.*, 2021), which can produce underestimates of tree diameter when summing ring widths together to calculate DBH. However, our method for scaling chronology carbon increments to the stand should implicitly adjust for those underestimates. Likewise, there may be uncertainties related to mortality, allometry, and sampling design (Alexander *et al.*, 2018), though again we note that there is no reason why these would directionally bias our AWCI : GPP estimates. We highlight that our method still produces estimates of AWCI : GPP that are within the bounds of previous estimates, while also allowing us to generate the large number of AWCI : GPP data necessary to elucidate the drivers of its variability over space and time (which is not possible with single-site estimates or low-frequency surveys).

## Drivers of AWCI, GPP, and AWCI : GPP

We next sought to uncover drivers of interannual variability in AWCI, GPP, and AWCI : GPP. First, we built random forest models with growing season climate anomalies and LAI to quantify the degree to which these quantities were associated with interannual climate variability. The models were not strong predictors of AWCI (mean $R^2$ between testing and training datasets = 0.20) or AWCI : GPP (Fig. 4; $R^2$ = 0.26). Solar radiation was the most predictive variable, with lower incoming radiation levels increasing AWCI and AWCI : GPP (Figs S3, S4). This could be due to light competition inducing allocation to aboveground growth, or increased cloudiness alleviating water stress at some sites. The models built to predict GPP were much more successful, however (Fig. S5; $R^2$ = 0.61), likely because the controls over GPP are less complex and more instantaneous than those for AWCI. LAI was the variable that most increased the predictive ability of the GPP model, with higher LAI values associated with higher annual GPP, likely due to the strong linkage between canopy density and carbon uptake across space (Hoek Van Dijke *et al.*, 2020).

Since most of the variability in AWCI, GPP, and AWCI : GPP occurred across sites, we then built random forest models to predict these processes using mean site climate, mean LAI, and stand basal area (Fig. 4). These models were much more successful at predicting AWCI ($R^2$ = 0.61), GPP ($R^2$ = 0.85), and

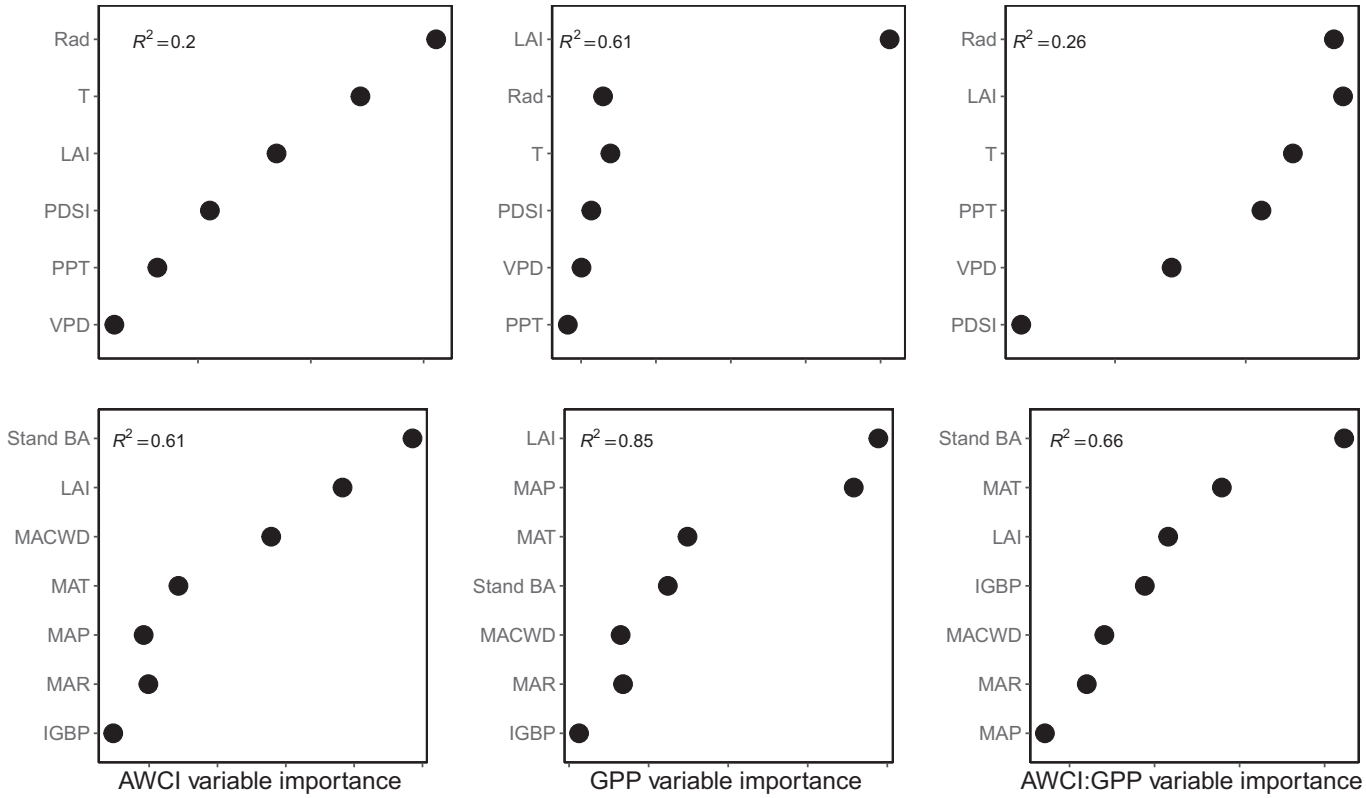


**Fig. 4** Variable importance plots documenting the importance of scaled annual climate, mean site climate, and forest structural variables on the prediction of aboveground woody carbon increment (AWCI), gross primary productivity (GPP), and AWCI : GPP. Predictors include the following: incoming shortwave radiation (Rad), growing season temperature (T), growing season leaf area index (LAI), growing season Palmer Drought Severity Index (PDSI), growing season precipitation (PPT), growing season vapor pressure deficit (VPD), mean annual climatic water deficit (MACWD), stand basal area (Stand BA), mean annual temperature (MAT), mean annual leaf area index (LAI), mean annual precipitation (MAP), mean annual incoming shortwave radiation (MAR), and IGBP classification. $R^2$ indicates the mean $R^2$ of the training model when applied to the testing data across 100 random iterations. The top row of panels represents predictors that vary interannually, while the bottom row of panels represents mean site predictor values.

AWCI : GPP ($R^2$ = 0.66). Variable importance plots revealed that stand density and LAI were critical variables for AWCI and GPP model predictive ability, respectively, with denser forests/canopies being associated with higher AWCI and GPP (Figs S6, S7). AWCI : GPP, however, was highest at colder stands with low LAI and high basal area (Fig. S8). This finding adds to existing evidence that high biomass forests are likely to allocate higher percentages of photosynthate to growth (Vicca *et al.*, 2012), while the high allocation of carbon to growth in low leaf area forests could be due to known allometric trade-offs (Chen *et al.*, 2013) that arise due to the nature of competition and resource availability in forests. While there were slight differences across processes, hydroclimatic drivers were also important model predictors. For example, AWCI was highest at wetter sites, while GPP was highest at sites with intermediate rainfall. This may reflect how water availability consistently enhances woody biomass production, though very wet sites might experience reductions in GPP due to direct suppression of photosynthesis or increased cloud cover at wetter sites. The small role of IGBP vegetation class in these models is notable and likely indicates that the variability in these processes is controlled by the broad climatic factors already included in the model, rather than intrinsic differences in vegetation type (Barnes *et al.*, 2021). We do caution that these analyses do not indicate causality and are instead intended to provide fruitful avenues for further research. Promisingly, though, the fact that the fraction of GPP allocated to AWCI was best predicted by broad site-level climate and structure hints that developing a mechanistic representation of this allocation may be tractable.

While it is well known that severe water stress suppresses both woody tree growth and photosynthesis, we further hypothesized that these climate extremes also might decrease AWCI : GPP, given that (1) radial growth is likely a minor allocation priority for a tree during these times (Kannenberg *et al.*, 2019a,b; Wei *et al.*, 2024), and (2) growth processes are usually more sensitive to water stress than photosynthesis (Muller *et al.*, 2011; Peters *et al.*, 2021). To test this, we identified drought years (PDSI < −3) and pluvial years (PDSI > 3) in our dataset, and compared AWCI : GPP during those years with climatically normal years. Pluvial years did not significantly alter the fraction of GPP allocated to AWCI, relative to normal years. However, severe drought significantly ($P$ < 0.05) decreased AWCI : GPP by 33% relative to normal years (Fig. 5). Furthermore, this effect persisted for 3 yr following the drought event ($P$ < 0.05), with reductions of

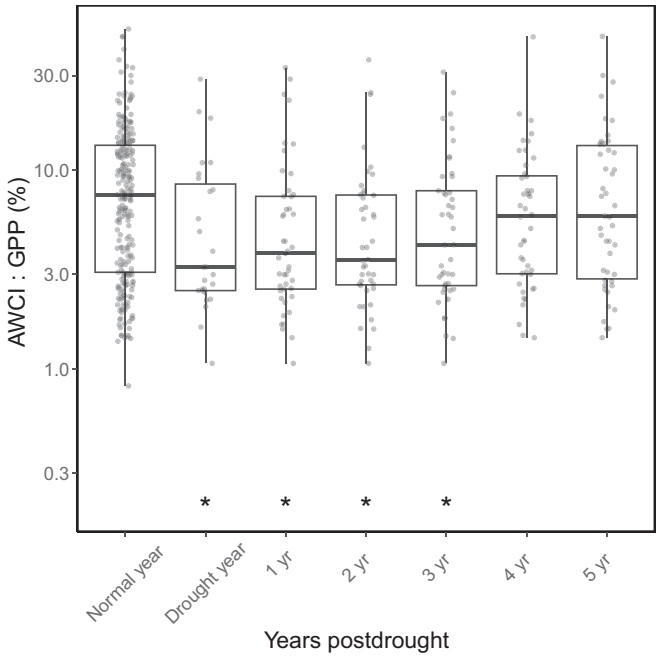


**Fig. 5** AWCI : GPP during climatically normal years, drought years, and up to 5 yr postdrought. Asterisks indicate statistical significance via *t*-test ($P < 0.05$) between drought years (or years following drought) and climatically normal years. Boxes represent the median +-/ the interquartile range, while the "whiskers" indicate the maximum/minimum non-noutlier values. The *y*-axis is plotted on a log scale for clarity, but see Supporting Information Fig. S11 for a nonlog-transformed version. AWCI, aboveground woody carbon increment; GPP, gross primary productivity.

30% in postdrought year 1, 34% in year 2, and 29% in year 3. These results held regardless of whether we considered all climatically normal years in our dataset vs only considering normal years at sites that experienced severe droughts or pluvials. This result is consistent with previous research indicating that 'drought legacy effects' in tree rings commonly last for *c.* 2–4 yr (Anderegg *et al.*, 2015), while GPP tends to recover quickly (Kannenberg *et al.*, 2020). The ramifications for the carbon cycle could be significant. In forests that are projected to experience accelerating and intensifying drought (McDowell *et al.*, 2020), this may indicate that forests will increasingly allocate carbon to pools with much lower residence times, thus impacting long-term carbon sequestration (Kannenberg *et al.*, 2022).

## Limitations

Our method, developed to complement a large database of tree-ring chronologies at flux tower sites, has several caveats and uncertainties. For example, (1) allometric equations can be highly uncertain across sites (as can estimates of foliar allocation), (2) many times tree-ring chronologies are not collected in a randomized or systematic manner and thus ignore suppressed or understory trees (Nehrbass-Ahles *et al.*, 2014), (3) there may be interspecific and interannual fluctuations in wood density not accounted for here (Babst *et al.*, 2014b), and (4) stand basal area estimates used a number of different methodologies and may be uncertain. Allometric equations also do not account for branch turnover, which can increase estimates of woody biomass production by *c.* 16% (Lim *et al.*, 2024). We also lack consistent data on site fertility across time and space, which may be an important driver of variability in AWCI : GPP (Vicca *et al.*, 2012). Our estimates of AWCI : GPP, which lie on the lower end of previously published estimates, likely reflect some of these uncertainties. To reduce these uncertainties, future tree-ring chronology development at flux tower sites should incorporate measurements of tree diameter along with stand surveys with either fixed area or randomized sample designs. Estimating growth from smaller trees would also be useful, as they can make up a sizeable portion of productivity in some forests (Piponiot *et al.*, 2022, though see Babst *et al.*, 2014a), as would estimates of branch turnover (Lim *et al.*, 2024) and carbon allocation to bark (Neumann & Lawes, 2021). Despite this, our approach can generate estimates of AWCI that are in line with other published estimates, and due to the limited data collection requirements (i.e. only tree-ring chronologies, species composition estimates, and stand basal area) can be easily implemented and applied across a wide range of flux tower sites. Accurate and widespread AWCI estimates are exceedingly useful for improving our ability to track the flow and permanence of carbon in forest ecosystems and are thus highly relevant for quantifying the efficacy of forest-based climate solutions.

## Conclusions

Scaling ecological dynamics from individual trees to whole ecosystem processes is a critical frontier in ecological, dendrochronological, and carbon cycle research (Babst *et al.*, 2018). By developing a method to generate chronologies of whole-forest aboveground woody carbon derived from tree-ring samples, we facilitate direct comparisons between historical records of tree growth and ecosystem carbon uptake. We found that AWCI was a relatively small and decoupled fraction of GPP that varied considerably across space and somewhat through time. Notably, most of this variation was due to differences in site climate and stand structure, which offers clues toward better representing this fraction in vegetation models and assessments of forest carbon sequestration. Ultimately, our results highlight some vital points for the ecological community: (1) that past and projected increases in GPP do not necessarily translate directly into increased long-lived woody biomass as simply as many allocation schemes suggest, (2) we need more field-based studies on carbon allocation in mature trees, especially high-resolution sampling via automated dendrometers, xylogenesis, LAI measurements, ground-based LiDAR, or similar, and (3) care should be taken when quantifying ecological phenomena using only tree rings or flux towers in isolation. Approaches where multiple carbon cycle processes are investigated concomitantly hold great promise toward accurately quantifying variability in forest carbon cycling/storage (Novick *et al.*, 2022) and improving projections of forest responses to current and ongoing changes in climate (Babst *et al.*, 2021), as do recent optimality-based improvements in the modeling of carbon allocation (Trugman *et al.*, 2018; Potkay *et al.*, 2021).

## Acknowledgements

We would like to extend our sincerest thanks to those who contributed tree-ring data to the Cabon *et al.* (2022) dataset, as well at the AmeriFlux and FLUXNET PIs who constructed and maintained the flux tower sites used in this study. SAK was supported by the US National Science Foundation Division of Environmental Biology award #2331162 and US National Science Foundation Dynamics of Integrated Socio-Environmental systems award #2408954. MPD and MRJ were supported by the US National Science Foundation EPSCoR award #2131853. MPD was also supported by the University of Iowa's James Van Allen Fellowship.

## Competing interests

None declared.

## Author contributions

SAK, MLB, MPD and MRJ conceptualized the study, while SAK and AC amassed the dataset. SAK conducted analyses with input from FB, MLB, AC, MPD, MRJ, and WRLA. SAK wrote the initial draft, which was edited and revised by FB, MLB, AC, MPD, MRJ, and WRLA.

## ORCID

Steven A. Kannenberg https://orcid.org/0000-0002-4097-9140

## Data availability

All data are present either in Cabon *et al.* (2022) via doi: 10.5061/dryad.15dv41nzt or in Table S1.

## References

**Alexander MR, Rollinson CR, Babst F, Trouet V, Moore DJP. 2018.** Relative influences of multiple sources of uncertainty on cumulative and incremental tree-ring-derived aboveground biomass estimates. *Trees* **32**: 265–276.

**Anderegg WRL, Schwalm C, Biondi F, Camarero JJ, Koch G, Litvak M, Ogle K, Shaw D, Shevliakova E, Williams AP *et al.* 2015.** Pervasive drought legacies in forest ecosystems and their implications for carbon cycle models. *Science* **349**: 528–532.

**Babst F, Bodesheim P, Charney N, Friend AD, Girardin MP, Klesse S, Moore DJP, Seftigen K, Björklund J, Bouriaud O *et al.* 2018.** When tree rings go global: Challenges and opportunities for retro- and prospective insight. *Quaternary Science Reviews* **197**: 1–20.

**Babst F, Bouriaud O, Alexander R, Trouet V, Frank D. 2014a.** Toward consistent measurements of carbon accumulation: a multi-site assessment of biomass and basal area increment across Europe. *Dendrochronologia* **32**: 153–161.

**Babst F, Bouriaud O, Papale D, Gielen B, Janssens IA, Nikinmaa E, Ibrom A, Wu J, Bernhofer C, Köstner B *et al.* 2014b.** Above-ground woody carbon sequestration measured from tree rings is coherent with net ecosystem productivity at five eddy-covariance sites. *New Phytologist* **201**: 1289–1303.

**Babst F, Friend AD, Karamihalaki M, Wei J, von Arx G, Papale D, Peters RL. 2021.** Modeling ambitions outpace observations of forest carbon allocation. *Trends in Plant Science* **26**: 210–219.

**Barnes ML, Biederman JA, Farella MM, Scott RL, Moore DJP, Ponce-Campos GE, Biederman J, MacBean N, Litvak ME, Breshears DD. 2021.** Improved dryland carbon flux predictions with explicit consideration of water-carbon coupling. *Communications Earth & Environment* **2**: 248.

**Bonan GB. 2008.** Forests and climate change: forcings, feedbacks, and the climate benefits of forests. *Science* **320**: 1444–1449.

**Brüggemann N, Gessler A, Kayler Z, Keel SG, Badeck F, Barthel M, Boeckx P, Buchmann N, Brugnoli E, Esperschütz J *et al.* 2011.** Carbon allocation and carbon isotope fluxes in the plant-soil-atmosphere continuum: a review. *Biogeosciences* **8**: 3457–3489.

**Brzostek ER, Dragoni D, Schmid HP, Rahman AF, Sims D, Wayson CA, Johnson DJ, Phillips RP. 2014.** Chronic water stress reduces tree growth and the carbon sink of deciduous hardwood forests. *Global Change Biology* **20**: 2531–2539.

**Cabon A, Ameztegui A, Anderegg WRL, Martínez-Vilalta J, De Cáceres M. 2024.** Probing the interplay of biophysical constraints and photosynthesis to model tree growth. *Agricultural and Forest Meteorology* **345**: 109852.

**Cabon A, Kannenberg S, Arain A, Babst F, Baldocchi D, Belmecheri S, Delpierre N, Guerrieri R, Maxwell JT, McKenzie S *et al.* 2022.** Cross-biome synthesis of source versus sink limits to tree growth. *Science* **376**: 758–761.

**Campioli M, Gielen B, Göckede M, Papale D, Bouriaud O, Granier A. 2011.** Temporal variability of the NPP–GPP ratio at seasonal and interannual time scales in a temperate beech forest. *Biogeosciences* **8**: 2481–2492.

**Carvalhais N, Forkel M, Khomik M, Bellarby J, Jung M, Migliavacca M, Mu M, Saatchi S, Santoro M, Thurner M *et al.* 2014.** Global covariation of carbon turnover times with climate in terrestrial ecosystems. *Nature* **514**: 213–217.

**Chen G, Yang Y, Robinson D. 2013.** Allocation of gross primary production in forest ecosystems: allometric constraints and environmental responses. *New Phytologist* **200**: 1176–1186.

**Dannenberg MP, Song C, Wise EK, Pederson N, Bishop DA. 2020.** Delineating environmental stresses to primary production of U.S. Forests from tree rings: effects of climate seasonality, soil, and topography. *Journal of Geophysical Research: Biogeosciences* **125**: e2019JG005499.

**Delpierre N, Berveiller D, Granda E, Dufrêne E. 2016.** Wood phenology, not carbon input, controls the interannual variability of wood growth in a temperate oak forest. *New Phytologist* **210**: 459–470.

**DeLucia EH, Drake JE, Thomas RB, Gonzalez-Meler M. 2007.** Forest carbon use efficiency: is respiration a constant fraction of gross primary production? *Global Change Biology* **13**: 1157–1167.

**Dormann CF, Elith J, Bacher S, Buchmann C, Carl G, Carré G, Marquéz JRG, Gruber B, Lafourcade B, Leitão PJ *et al.* 2013.** Collinearity: a review of methods to deal with it and a simulation study evaluating their performance. *Ecography* **36**: 27–46.

**Dow C, Kim AY, D'Orangeville L, Gonzalez-Akre EB, Helcoski R, Herrmann V, Harley GL, Maxwell JT, McGregor IR, McShea WJ *et al.* 2022.** Warm springs alter timing but not total growth of temperate deciduous trees. *Nature* **608**: 552–557.

**Dye A, Plotkin AB, Bishop D, Pederson N, Poulter B, Hessl A. 2016.** Comparing tree-ring and Permanent plot estimates of aboveground net primary production in three eastern U.S. forests. *Ecosphere* **7**: 1–13.

**Falster DS, Duursma RA, Ishihara MI, Barneche DR, FitzJohn RG, Vårhammar A, Aiba M, Ando M, Anten N, Aspinwall MJ *et al.* 2015.** BAAD: a biomass and allometry database for woody plants. *Ecology* **96**: 1445.

**Fatichi S, Pappas C, Zscheischler J, Leuzinger S. 2019.** Modelling carbon sources and sinks in terrestrial vegetation. *New Phytologist* **221**: 652–668.

**Finzi AC, Giasson M, Barker Plotkin AA, Aber JD, Boose ER, Davidson EA, Dietze MC, Ellison AM, Frey SD, Goldman E *et al.* 2020.** Carbon budget of the Harvard Forest Long-Term Ecological Research site: pattern, process, and response to global change. *Ecological Monographs* **90**: e01423.

**Friend AD, Lucht W, Rademacher TT, Keribin R, Betts R, Cadule P, Ciais P, Clark DB, Dankers R, Falloon PD *et al.* 2014.** Carbon residence time dominates uncertainty in terrestrial vegetation responses to future climate and atmospheric $CO_2$. *Proceedings of the National Academy of Sciences, USA* **111**: 3280–3285.

**Gonzalez-Akre E, Piponiot C, Lepore M, Herrmann V, Lutz JA, Baltzer JL, Dick CW, Gilbert GS, He F, Heym M *et al.* 2022.** *ALLODB*: an R package for

biomass estimation at globally distributed extratropical forest plots. *Methods in Ecology and Evolution* **13**: 330–338.

**Greenwell B. 2017.** PDP: an R package for constructing partial dependence plots. *R Journal* **9**: 421–436.

**Guillemot J, Martin-StPaul NK, Dufrêne E, François C, Soudani K, Ourcival JM, Delpierre N. 2015.** The dynamic of the annual carbon allocation to wood in European tree species is consistent with a combined source–sink limitation of growth: implications for modelling. *Biogeosciences* **12**: 2773–2790.

**Hartmann H, Bahn M, Carbone M, Richardson AD. 2020.** Plant carbon allocation in a changing world – challenges and progress: introduction to a Virtual Issue on carbon allocation: introduction to a virtual issue on carbon allocation. *New Phytologist* **227**: 981–988.

**Hoek Van Dijke AJ, Mallick K, Schlerf M, Machwitz M, Herold M, Teuling AJ. 2020.** Examining the link between vegetation leaf area and land–atmosphere exchange of water, energy, and carbon fluxes using FLUXNET data. *Biogeosciences* **17**: 4443–4457.

**Hsiao TC. 1973.** Plant responses to water stress. *Annual Review of Plant Physiology* **24**: 519–570.

**Ikawa H, Nakai T, Busey RC, Kim Y, Kobayashi H, Nagai S, Ueyama M, Saito K, Nagano H, Suzuki R *et al.* 2015.** Understory $CO_2$, sensible heat, and latent heat fluxes in a black spruce forest in interior Alaska. *Agricultural and Forest Meteorology* **214–215**: 80–90.

**Kannenberg SA, Cabon A, Babst F, Belmecheri S, Delpierre N, Guerrieri R, Maxwell JT, Meinzer FC, Moore DJP, Pappas C *et al.* 2022.** Drought-induced decoupling between carbon uptake and tree growth impacts forest carbon turnover time. *Agricultural and Forest Meteorology* **322**: 108996.

**Kannenberg SA, Maxwell JT, Pederson N, D'Orangeville L, Ficklin DL, Phillips RP. 2019a.** Drought legacies are dependent on water table depth, wood anatomy and drought timing across the eastern US. *Ecology Letters* **22**: 119–127.

**Kannenberg SA, Novick KA, Alexander MR, Maxwell JT, Moore DJP, Phillips RP, Anderegg WRL. 2019b.** Linking drought legacy effects across scales: From leaves to tree rings to ecosystems. *Global Change Biology* **25**: 2978–2992.

**Kannenberg SA, Schwalm CR, Anderegg WRL. 2020.** Ghosts of the past: how drought legacy effects shape forest functioning and carbon cycling. *Ecology Letters* **23**: 891–901.

**Kattge J, Bönisch G, Díaz S, Lavorel S, Prentice IC, Leadley P, Tautenhahn S, Werner GDA, Aakala T, Abedi M *et al.* 2020.** TRY plant trait database – enhanced coverage and open access. *Global Change Biology* **26**: 119–188.

**Keenan TF, Gray J, Friedl MA, Toomey M, Bohrer G, Hollinger DY, Munger JW, O'Keefe J, Schmid HP, Wing IS *et al.* 2014.** Net carbon uptake has increased through warming-induced changes in temperate forest phenology. *Nature Climate Change* **4**: 598–604.

**Körner C. 2015.** Paradigm shift in plant growth control. *Current Opinion in Plant Biology* **25**: 107–114.

**Liaw A, Wiener M. 2002.** Classification and regression by RANDOMFOREST. *R News* **2**: 18–22.

**Lim H, Medvigy D, Mäkelä A, Kim D, Albaugh TJ, Knier A, Blaško R, C. Campoe O, Deshar R, Franklin O *et al.* 2024.** Overlooked branch turnover creates a widespread bias in forest carbon accounting. *Proceedings of the National Academy of Sciences, USA* **121**: e2401035121.

**Litton CM, Raich JW, Ryan MG. 2007.** Carbon allocation in forest ecosystems. *Global Change Biology* **13**: 2089–2109.

**Lockwood BR, Maxwell JT, Robeson SM, Au TF. 2021.** Assessing bias in diameter at breast height estimated from tree rings and its effects on basal area increment and biomass. *Dendrochronologia* **67**: 125844.

**Loescher HW, Law BE, Mahrt L, Hollinger DY, Campbell J, Wofsy SC. 2006.** Uncertainties in, and interpretation of, carbon flux estimates using the eddy covariance technique. *Journal of Geophysical Research: Atmospheres* **111**: 2005JD006932.

**McDowell NG, Allen CD, Anderson-Teixeira K, Aukema BH, Bond-Lamberty B, Chini L, Clark JS, Dietze M, Grossiord C, Hanbury-Brown A *et al.* 2020.** Pervasive shifts in forest dynamics in a changing world. *Science* **368**(6494): eaaz9463.

**McKenzie SM, Pisaric MFJ, Arain MA. 2021.** Comparison of tree-ring growth and eddy covariance-based ecosystem productivities in three different-aged pine plantation forests. *Trees* **35**: 583–595.

**Merganičová K, Merganič J, Lehtonen A, Vacchiano G, Sever MZO, Augustynczik ALD, Grote R, Kyselová I, Mäkelä A, Yousefpour R *et al.* 2019.** Forest carbon allocation modelling under climate change (A Polle, Ed.). *Tree Physiology* **39**: 1937–1960.

**Misson L, Baldocchi DD, Black TA, Blanken PD, Brunet Y, Curiel Yuste J, Dorsey JR, Falk M, Granier A, Irvine MR *et al.* 2007.** Partitioning forest carbon fluxes with overstory and understory eddy-covariance measurements: A synthesis based on FLUXNET data. *Agricultural and Forest Meteorology* **144**: 14–31.

**Muller B, Pantin F, Genard M, Turc O, Freixes S, Piques M, Gibon Y. 2011.** Water deficits uncouple growth from photosynthesis, increase C content, and modify the relationships between C and growth in sink organs. *Journal of Experimental Botany* **62**: 1715–1729.

**Nehrbass-Ahles C, Babst F, Klesse S, Nötzli M, Bouriaud O, Neukom R, Dobbertin M, Frank D. 2014.** The influence of sampling design on tree-ring-based quantification of forest growth. *Global Change Biology* **20**: 2867–2885.

**Neumann M, Lawes MJ. 2021.** Quantifying carbon in tree bark: the importance of bark morphology and tree size. *Methods in Ecology and Evolution* **12**: 646–654.

**Novick KA, Metzger S, Anderegg WRL, Barnes M, Cala DS, Guan K, Hemes KS, Hollinger DY, Kumar J, Litvak M *et al.* 2022.** Informing Nature-based Climate Solutions for the United States with the best-available science. *Global Change Biology* **28**: 3778–3794.

**O'Sullivan M, Friedlingstein P, Sitch S, Anthoni P, Arneth A, Arora VK, Bastrikov V, Delire C, Goll DS, Jain A *et al.* 2022.** Process-oriented analysis of dominant sources of uncertainty in the land carbon sink. *Nature Communications* **13**: 4781.

**Pan Y, Birdey RA, Fang J, Houghton R, Kauppi PE, Kurz WA, Phillips OL, Shcidenko A, Lewis SL, Canadell JG *et al.* 2011.** A large and persistent carbon sink in the world's forests. *Science* **333**: 988–993.

**Pappas C, Maillet J, Rakowski S, Baltzer JL, Barr AG, Black TA, Fatichi S, Laroque CP, Matheny AM, Roy A *et al.* 2020.** Aboveground tree growth is a minor and decoupled fraction of boreal forest carbon input. *Agricultural and Forest Meteorology* **290**: 108030.

**Peters RL, Steppe K, Cuny HE, De Pauw DJW, Frank DC, Schaub M, Rathgeber CBK, Cabon A, Fonti P. 2021.** Turgor – a limiting factor for radial growth in mature conifers along an elevational gradient. *New Phytologist* **229**: 213–229.

**Piponiot C, Anderson-Teixeira KJ, Davies SJ, Allen D, Bourg NA, Burslem DFRP, Cárdenas D, Chang-Yang C, Chuyong G, Cordell S *et al.* 2022.** Distribution of biomass dynamics in relation to tree size in forests across the world. *New Phytologist* **234**: 1664–1677.

**Potkay A, Trugman AT, Wang Y, Venturas MD, Anderegg WRL, Mattos CRC, Fan Y. 2021.** Coupled whole-tree optimality and xylem hydraulics explain dynamic biomass partitioning. *New Phytologist* **230**: 2226–2245.

**Prescott CE, Grayston SJ, Helmisaari HS, Kaštovská E, Körner C, Lambers H, Meier IC, Millard P, Ostonen I. 2020.** Surplus carbon drives allocation and plant–soil interactions. *Trends in Ecology & Evolution* **35**: 1110–1118.

**Pugh TAM, Rademacher T, Shafer SL, Steinkamp J, Barichivich J. 2020.** Understanding the uncertainty in global forest carbon turnover. *Biogeosciences* **17**: 3961–3989.

**R Core Team. 2023.** *R: a language and environment for statistical computing.* Vienna, Austria: R Foundation for Statistical Computing.

**Rocha AV, Goulden ML, Dunn AL, Wofsy SC. 2006.** On linking interannual tree ring variability with observations of whole-forest $CO_2$ flux. *Global Change Biology* **12**: 1378–1389.

**Rog I, Hilman B, Fox H, Yalin D, Qubaja R, Klein T. 2024.** Increased belowground tree carbon allocation in a mature mixed forest in a dry versus a wet year. *Global Change Biology* **30**: e17172.

**Teets A, Fraver S, Hollinger DY, Weiskittel AR, Seymour RS, Richardson AD. 2018a.** Linking annual tree growth with eddy-flux measures of net ecosystem productivity across twenty years of observation in a mixed conifer forest. *Agricultural and Forest Meteorology* **249**: 479–487.

**Teets A, Fraver S, Weiskittel AR, Hollinger DY. 2018b.** Quantifying climate-growth relationships at the stand level in a mature mixed-species conifer forest. *Global Change Biology* **24**: 3587–3602.

**Teets A, Moore DJP, Alexander MR, Blanken PD, Bohrer G, Burns SP, Carbone MS, Ducey MJ, Fraver S, Gough CM *et al.* 2022.** Coupling of tree

growth and photosynthetic carbon uptake across six North American Forests. *Journal of Geophysical Research: Biogeosciences* **127**: e2021JG006690.

**Trugman AT, Detto M, Bartlett MK, Medvigy D, Anderegg WRL, Schwalm C, Schaffer B, Pacala SW. 2018.** Tree carbon allocation explains forest drought-kill and recovery patterns. *Ecology Letters* **21**: 1552–1560.

**Tuck SL, Phillips HRP, Hintzen RE, Scharlemann JPW, Purvis A, Hudson LN. 2014.** MODISTools - downloading and processing MODIS remotely sensed data in R. *Ecology and Evolution* **4**: 4658–4668.

**Vicca S, Luyssaert S, Peñuelas J, Campioli M, Chapin FS, Ciais P, Heinemeyer A, Högberg P, Kutsch WL, Law BE *et al.* 2012.** Fertile forests produce biomass more efficiently. *Ecology Letters* **15**: 520–526.

**Walker AP, De Kauwe MG, Bastos A, Belmecheri S, Georgiou K, Keeling RF, McMahon SM, Medlyn BE, Moore DJP, Norby RJ *et al.* 2020.** Integrating the evidence for a terrestrial carbon sink caused by increasing atmospheric $CO_2$. *New Phytologist* **229**: 2413–2445.

**Wei J, Von Arx G, Fan Z, Ibrom A, Mund M, Knohl A, Peters RL, Babst F. 2024.** Drought alters aboveground biomass production efficiency: Insights from two European beech forests. *Science of the Total Environment* **919**: 170726.

## Supporting Information

Additional Supporting Information may be found online in the Supporting Information section at the end of the article.

**Fig. S1** Map of sites.

**Fig. S2** Relationships between AWCI derived from this study and Teets *et al.* (2022).

**Fig. S3** Smoothed partial dependence plots documenting the dependence between AWCI and various scaled annual climate variables.

**Fig. S4** Smoothed partial dependence plots documenting the dependence between AWCI : GPP and various scaled annual climate variables.

**Fig. S5** Smoothed partial dependence plots documenting the dependence between GPP and various scaled annual climate variables.

**Fig. S6** Smoothed partial dependence plots documenting the dependence between AWCI and various mean stand variables.

**Fig. S7** Smoothed partial dependence plots documenting the dependence between GPP and various mean stand variables.

**Fig. S8** Smoothed partial dependence plots documenting the dependence between AWCI : GPP and various mean stand variables.

**Fig. S9** Fig. 2 but with nonlog-transformed axes.

**Fig. S10** Fig. 3 but with nonlog-transformed axes.

**Fig. S11** Fig. 5 but with nonlog-transformed axes.

**Table S1** Sites used in the study along with various metadata, including: DOI, latitude and longitude, elevation, IGBP, MAT, MAP, MACWD, MAR, stand basal area, and the source for the basal area estimates.

Please note: Wiley is not responsible for the content or functionality of any Supporting Information supplied by the authors. Any queries (other than missing material) should be directed to the *New Phytologist* Central Office.